

RSC Advances



This is an *Accepted Manuscript*, which has been through the Royal Society of Chemistry peer review process and has been accepted for publication.

Accepted Manuscripts are published online shortly after acceptance, before technical editing, formatting and proof reading. Using this free service, authors can make their results available to the community, in citable form, before we publish the edited article. This *Accepted Manuscript* will be replaced by the edited, formatted and paginated article as soon as this is available.

You can find more information about *Accepted Manuscripts* in the [Information for Authors](#).

Please note that technical editing may introduce minor changes to the text and/or graphics, which may alter content. The journal's standard [Terms & Conditions](#) and the [Ethical guidelines](#) still apply. In no event shall the Royal Society of Chemistry be held responsible for any errors or omissions in this *Accepted Manuscript* or any consequences arising from the use of any information it contains.

Synthesis and adsorption property of hydrophilic-hydrophobic macroporous crosslinked poly(methyl acryloyl diethylenetriamine)/poly(divinylbenzene) (PMADETA/PDVB) interpenetrating polymer networks (IPNs)

Hebing Li, Zhenyu Fu, Li Yang, Chong Yan, Limiao Chen, Jianhan Huang*, You-Nian Liu

College of Chemistry and Chemical Engineering, Central South University, Changsha, Hunan 410083, China

*Corresponding author. E-mail address: jianhanhuang@csu.edu.cn

Abstract: Hydrophilic-hydrophobic macroporous crosslinked poly(methyl acryloyl diethylenetriamine)/poly(divinylbenzene) (PMADETA/PDVB) interpenetrating polymer networks (IPNs) were prepared, characterized and evaluated for adsorption of salicylic acid from aqueous solution. PMADETA/PDVB IPNs were prepared by filling PDVB networks in the pores of PGMA networks according to a IPNs technology and an amination reaction of PGMA/PDVB IPNs with diethylenetriamine (DETA). The structure of PMADETA/PDVB IPNs was characterized by Fourier transform infrared spectroscopy (FT-IR), N_2 adsorption-desorption isotherms and chemical analysis. PMADETA/PDVB IPNs had a very large equilibrium adsorption capacity to salicylic acid and the equilibrium adsorption capacity was measured to be 196.4 mg/g at an equilibrium concentration of 100 mg/L. The Freundlich model was more appropriate for fitting the equilibrium data than the Langmuir model and the adsorption was shown to be an exothermic and spontaneous process. The adsorption reached equilibrium within 200 min and the pseudo-second-order rate equation characterized the kinetic data better than the pseudo-first-order rate equation. At an initial concentration of 1035 mg/L and a flow rate of 84 mL/h, the breakthrough and saturated capacities were 75.02 and 159.53 mg/mL wet resin, respectively, and the resin column could be completely regenerated and repeatedly by 0.01 mol/L of NaOH (w/v) and 20% of ethanol (v/v).

Keywords: Interpenetrating polymer networks (IPNs); poly(methyl acryloyl diethylenetriamine) (PMADETA); poly(divinylbenzene) (PDVB); adsorption; salicylic acid

1. Introduction

Salicylic acid is a popular ingredient in many over-the-counter products. It is frequently found in lotions and creams, cleansers, medicated treatment pads and solutions. In particular, salicylic acid is widely used as an important pharmaceutical intermediate for production of medicine (aspirin), and it can be applied for preservation of food, preservatives of glue and brightener of cosmetic, hence production amount of salicylic acid is very huge [1, 2]. However, salicylic acid can cause stinging, burning, skin irritation and serious environmental problems [3-5]. Even if with a low concentration to 10^{-4} M, it will affect the natural growth of plants [6]. Recently, wastewater containing salicylic acid has been identified as a water pollutant for its ecotoxicity in water, which originates mainly from manufacturing activities of salicylic acid [7]. Generally, the pharmaceutical concentrations of salicylic acid from the effluents were in the range of 10-1000 ng/L, the detected concentration of salicylic acid was about 2098 ng/L in the river of Chu Chiang Delta region in China [8]. As a result, efficient removal of salicylic acid from aqueous solution has received many attentions in recent years.

A lot of methods and technologies including catalysis, membrane separation, oxidation, extraction and adsorption have been developed for removal of aromatic compounds [9-15], among which adsorption is proved to the most simple and efficient method [16-18]. With respect to activated carbon, synthetic resins are increasingly employed for efficient removal and recovery of aromatic compounds from wastewater due to their stable physicochemical structure, diverse chemical structure, controllable pore structure and feasible regeneration property, and development of novel synthetic resins aimed at the molecular structure of the adsorbate remains a high priority and has attracted many interests in recent years [19-21]. In consideration of its molecular structure, salicylic acid has a hydrophobic benzene ring as well as hydrophilic phenolic hydroxyl and carboxyl groups. Moreover, there exists an intramolecular hydrogen bonding between the phenolic hydroxyl group and the carboxyl

group, which constitutes a planar hexatomic ring. Moreover, the newly formed planar hexatomic ring is relatively hydrophobic, making salicylic acid a well-balanced molecule with both of hydrophobic portion and hydrophilic portion. In 1970s, interpenetrating polymer networks (IPNs) were developed as a kind of novel polymeric materials for adsorption, and one of the important characteristics of IPNs is the force compatibility effect [22-24]. The chains of one polymer networks in the IPNs are physically tangled with another chains of the other polymer networks [25-27]. In addition to mutual physical entanglements, not any new chemical bond is formed between the two polymer networks in the IPNs. The strong phase separation liability will present between the hydrophobic and the hydrophilic polymer networks, and hence the hydrophobicity or the hydrophilicity of the two polymer networks composed of the IPNs is similar [28-30]. Moreover, it is a great challenge to prepare typical IPNs which contains both hydrophobic and hydrophilic polymer networks, and we have obtained hydrophobic-hydrophilic IPNs composed of polydivinylbenzene (PDVB) and polyacryl diethylenetriamine (PADETA) by filling polymethylacrylate (PMA) networks in the pores of PDVB networks according to a IPNs technology and a further amination reaction of PDVB/PMA IPNs [17, 18, 31], and it is proposed that the PDVB/PADETA IPNs is typical IPNs with both of hydrophobic networks and hydrophilic networks. They possess superior swelling and adsorption properties in hydrophobic-hydrophilic solvent (like benzyl alcohol) and the adsorbate (salicylic acid and anthranilic acid).

In this study, we developed a novel hydrophilic-hydrophobic IPNs composed of hydrophilic PMADETA and hydrophobic PDVB and used this novel IPNs for adsorption of salicylic acid from aqueous solution. For this purpose, firstly hydrophobic-hydrophobic macroporous crosslinked poly(glycidyl methacrylate)/poly(divinylbenzene) (PGMA/PDVB) IPNs was prepared by a typical IPNs technology. Then the first hydrophobic PGMA networks were transformed to the hydrophilic poly(methyl acryloyl diethylenetriamine) (PMADETA)

networks by an amination reaction, and hence the macroporous crosslinked hydrophilic-hydrophobic PMADETA/PDVB IPNs were achieved. After characterization of PMADETA/PDVB IPNs by Fourier transform infrared (FT-IR) spectroscopy, N₂ adsorption-desorption isotherms and other chemical analysis, the adsorption performance of PMADETA/PDVB IPNs toward salicylic acid were investigated in detail.

2. Experimental

2.1 Materials

GMA and DVB were used as the monomer in the polymerization, and they were firstly washed by 5% of NaOH (w/v) for three times and followed by de-ionized water. After the washing process, GMA and DVB were dried by anhydrous calcium chloride and kept in the refrigerator for 24 h before use. Benzoyl peroxide (BPO) employed as the initiator in the polymerization was refined by methanol before use. Salicylic acid, toluene, *n*-heptane, triallylisocyanurate (TAIC) and diethylenetriamine (DETA) were all analytical reagents and used without further purification.

2.2 Preparation of macroporous crosslinked PMADETA/PDVB IPNs

As shown in Scheme 1, macroporous crosslinked PMADETA/PDVB IPNs were prepared from macroporous crosslinked PGMA/PDVB IPNs by an amination reaction with DETA and the PGMA/PDVB IPNs was obtained by interpenetration of PDVB networks in PGMA networks. The macroporous crosslinked PGMA polymeric beads were prepared by a typical suspension polymerization of GMA and TAIC using toluene and *n*-heptane as the porogens. Toluene and *n*-heptane were 200% relative to the monomers (w/w) and the mass ratio between toluene and *n*-heptane was defined as 4:1. The obtained PGMA beads were swollen in the mixtures of DVB, BPO, toluene and *n*-heptane for 24 h and the mass ratio of PGMA to DVB was determined as 1:1. The swollen PGMA beads were filtered and added into 0.05% of

polyvinyl alcohol (PVA) aqueous solution (w/v). At a moderate stirring speed (190 rpm), the temperature of the reaction mixture was risen to 358 K and kept at this temperature for 12 h. The resultant PGMA/PDVB IPNs were chemically transformed to macroporous crosslinked PMADETA/PDVB IPNs by an amination reaction of PGMA/PDVB IPNs with DETA at 393 K for 15 h.

(Scheme 1 can be inserted here)

2.3 Characterization

FT-IR spectra of the resins were recorded on a Nicolet 510P Fourier transform infrared instrument in $500\text{-}4000\text{ cm}^{-1}$ with a resolution of 1.0 cm^{-1} . The Brunauer-Emmett-Teller (BET) surface area, pore volume and pore diameter distribution of the resins were determined by N_2 adsorption-desorption isotherms at 77 K using a Micromeritics Tristar 3000 surface area and porosity analyzer. The weak basic exchange capacity of the resins was measured according to the Ref [32].

2.4 Equilibrium and kinetic adsorption

The resins (about 0.1000 g) were mixed with 50 mL of salicylic acid at different initial concentrations. The initial concentrations of salicylic acid were pre-set to be 200.5, 401.0, 601.5, 802.0 and 1002.5 mg/L, respectively. The mixtures were then continuously shaken at a desired temperature (298, 308 and 318 K, respectively) for 8 h until equilibrium. To determine the equilibrium concentration of salicylic acid in aqueous solution, the working curve of the standard salicylic acid solution with different known concentrations was firstly measured by UV absorbency at a wavelength of 296.5 nm on a UV 2450 spectrophotometer, and a well fitted regression equation, $A=0.02528C+0.0096$, was obtained with a correlation coefficient R^2 of 0.9997. The absorbency of the residual salicylic acid solution adsorbed by the resin was then measured and the equilibrium concentration of salicylic acid, C_e (mg/L), was calculated based on the working curve, and the equilibrium adsorption capacity of salicylic acid on the resins

were calculated by conducting a mass balance of salicylic acid on the resins before and after the equilibrium. The kinetic curves for the adsorption of salicylic acid on the resins were similar to the equilibrium adsorption except that the adsorption capacity was determined in real time until equilibrium. The initial concentration of salicylic acid was pre-set to be 613.5 mg/L and the temperature was 298 K, respectively.

2.5 Dynamic adsorption and desorption

The resins were fully immersed in de-ionized water for 24 h and 8.6 mL (1 BV) wet resins were packed densely in a glass column to assemble a resin column. The salicylic acid at an initial concentration of 1035 mg/L was passed through the resin column at a fixed flow rate of 9.8 BV/h and the residual concentration of salicylic acid from the effluent was dynamically recorded until it reached the initial concentration. 0.01 mol/L of NaOH (w/v) and 20% of ethanol (v/v) was applied as the desorption solvent for the dynamic desorption. At a flow rate of 3.5 BV/h, the concentration of salicylic acid from the effluent was tested until it was about zero.

3. Results and discussion

3.1 Characterization of macroporous crosslinked PMADETA/PDVB IPNs

As shown in Table 1, after interpenetration of PDVB networks in PGMA networks, the particle size of the polymer remains to be 0.4-0.6 mm, while the BET surface area and pore volume increase from 64.00 m²/g and 0.3587 cm³/g (PGMA) to 271.3 m²/g and 0.7249 cm³/g (PGMA/PDVB IPNs), respectively, which may be from the fact that the pores of the PGMA networks are supported and filled by the PDVB networks. After the amination reaction of PGMA/PDVB IPNs with DETA, the BET surface area and pore volume further increase to 290.3 cm³/g and 0.8780 cm³/g, which may be resulted from the crosslinking of DETA between the PGMA chains.

(Table 1 can be inserted here)

Fig. 1 displays the FT-IR spectra of PGMA, PDVB, PMADETA, PGMA/PDVB IPNs and PMADETA/PDVB IPNs, respectively. It indicates that the FT-IR spectrum of PGMA/PDVB IPNs is completely superimposed by that of PGMA and PDVB. The strong vibrational band with frequency at 1728 cm^{-1} [33], which can be assigned to the C=O stretching of the ester carbonyl groups of PGMA, is emerged in the corresponding FT-IR spectrum of PGMA/PDVB IPNs. Additionally, the strong absorption bands at 1600 , 1496 and 1448 cm^{-1} , which are related to the C=C stretching of benzene ring of PDVB [34, 35], are also observed in the FT-IR spectrum of PGMA/PDVB IPNs. These results reveal that, in addition to mutual physical entanglements between the PGMA and PDVB networks, not any new chemical bonds are formed and the obtained polymer complex PGMA/PDVB is typical IPNs. After the amination of PGMA/PDVB IPNs with DETA, the strong vibrational band at 1728 cm^{-1} is sharply weakened, whereas a new moderate band appears at 1651 cm^{-1} in the FT-IR spectrum of PMADETA/PDVB IPNs, and this strong band may be concerned with the C=O stretching of the amide carbonyl groups [33]. Additionally, another new broad and strong vibration with frequency at 3429 cm^{-1} is also appeared in the FT-IR spectrum of PMADETA/PDVB IPNs, and this vibration may be assigned to the N-H stretching of the -NH-/-NH₂ groups or the O-H stretching of the hydroxyl groups [36-39]. Moreover, these related vibrational bands of the amide carbonyl groups appear in the FT-IR spectrum of PMADETA. The weak basic exchange capacity of PMADETA/PDVB IPNs was measured to be 3.479 mmol/g (Table 1), whereas those of PGMA and PGMA/PDVB IPNs were determined to be 0, which suggested that the PGMA networks of PGMA/PDVB IPNs were transformed to PMADETA networks and macroporous crosslinked PMADETA/PDVB IPNs was synthesized successfully.

(Fig. 1 can be inserted here)

3.2 Equilibrium adsorption

PMADETA/PDVB IPNs contain hydrophilic PMADETA networks as well as

hydrophobic PDVB networks in the polymer chains, which leads it to be both hydrophilic and hydrophobic, and it should have a relatively high adsorption affinity to the adsorbate with both of hydrophilic and hydrophobic portion. As a result, it is proposed that the adsorption of salicylic acid on PMADETA/PDVB IPNs should be very efficient as compared with the hydrophilic PMADETA as well as the hydrophobic PDVB.

The equilibrium adsorption isotherms of salicylic acid on PMADETA/PDVB IPNs were measured in comparison with PGMA, PGMA/PDVB IPNs as well as PMADETA and the results are displayed in Fig. 2. The equilibrium adsorption capacity of salicylic acid on PMADETA/PDVB IPNs was measured to be 232.4 mg/g, much larger than PGMA, PGMA/PDVB IPNs and PMADETA. As compared the equilibrium adsorption capacity of salicylic acid on synthetic resins with that on activated carbon, it was found that the equilibrium adsorption capacity of salicylic on synthetic resins was shown to be relatively smaller than that on activated carbon which was reported to be 351.0 mg/g [40] comparative with the crosslinked resins reported in Ref. [17] (230.7 mg/g), Ref. [31] (215.0 mg/g) and Ref. [41] (85.1 mg/g). However, activated carbon can not be used repeatedly, and the strength of activated carbon was weakened after using, which is much inferior to synthetic resins. In addition, PMADETA/PDVB IPNs possessed a greater BET surface area than PGMA and PGMA/PDVB IPNs, inducing a larger equilibrium adsorption capacity. In fact, the great superiority was perfectly embodied for the adsorption of salicylic acid on PMADETA/PDVB IPNs due to the perfect polarity matching between PMADETA/PDVB IPNs and salicylic acid. The hydrophilic PMADETA networks were inclined to approach the hydrophilic portion of salicylic acid (the phenolic hydroxyl and carboxyl groups) by static interaction or hydrogen bonding [42-45], the hydrophobic PDVB networks had a relative strong adsorption affinity to the hydrophobic portion of salicylic acid (the benzene ring and the newly formed hexatomic ring between the phenolic hydroxyl and carboxyl groups) via hydrophobic interaction or π - π

stacking [46-49]. Therefore, PMADETA/PDVB IPNs held a highly efficient adsorption to salicylic acid.

(Fig. 2 can be inserted here)

Fig. 3 is the equilibrium adsorption isotherms of salicylic acid on PMADETA/PDVB IPNs from aqueous solution with the temperature at 298, 308 and 318 K, respectively. It can be observed that the equilibrium adsorption capacity of salicylic acid PMADETA/PDVB IPNs increased with increasing of the equilibrium concentration, the temperature was unfavorable for the adsorption and a higher temperature induced a lower equilibrium adsorption capacity. Langmuir and Freundlich models were frequently adopted to describe the equilibrium adsorption process [50, 51], they can be arranged as:

$$\text{Langmuir model: } q_e = \frac{K_L C_e q_m}{1 + K_L C_e} \quad (\text{Eq. 1})$$

$$\text{Freundlich model: } q_e = K_F C_e^{1/n} \quad (\text{Eq. 2})$$

where q_e and q_m are the equilibrium and the maximum capacity of the adsorbates (mg/g), C_e is the equilibrium concentration of the adsorbates (mg/L), K_L is the Langmuir constant (L/mg), K_F ($[(\text{mg/g})(\text{L/mg})^{1/n}]$) and n is the Freundlich constant.

(Fig. 3 can be inserted here)

Both of the Langmuir and Freundlich models were applied for characterization of the equilibrium data and the corresponding characteristic parameters, q_m , K_L , K_F and n were summarized in Table 2. Table 2 indicated that the Freundlich model was more appropriate for characterizing the equilibrium data than the Langmuir model due to the much higher correlation coefficients ($R^2 > 0.99$). In addition, the n values for the adsorption was greater than 1, implying that the adsorption was a favorable process. The K_F values decreased with increasing of the temperature, suggesting that the adsorption affinity of salicylic acid on PMADETA/PDVB IPNs was less at a higher temperature.

(Table 2 can be inserted here)

As the equilibrium data could be correlated by the Freundlich model, the thermodynamic parameters for the adsorption can be obtained according to Eq. 3-Eq. 5 as follows [47, 52]:

$$\frac{d \ln C_e}{dT} = \frac{\Delta H}{RT^2} \quad (\text{Eq. 3})$$

$$\Delta G = -nRT \quad (\text{Eq. 4})$$

$$\Delta S = \frac{\Delta H - \Delta G}{T} \quad (\text{Eq. 5})$$

here ΔH is the isosteric adsorption enthalpy (kJ/mol), T is the temperature (K), R is the gas constant (8.314 J/(mol K)), ΔG is the adsorption free energy (kJ/mol), ΔS is the adsorption entropy (J/(mol·K)) and n is the Freundlich constant.

All the thermodynamic parameters such as ΔH , ΔG and ΔS were calculated and the results were summarized in Table 3. In addition, the ΔH of PMADETA/PDVB IPNs was calculated to be -53.11 kJ/mol with the temperature at 298 K and the value is larger than some other resins reported in Ref. [17] (-11.80 kJ/mol) and Ref. [31] (-14.60 kJ/mol).

(Table 3 can be inserted here)

3.3 Kinetic adsorption

Fig. 4 (a) displays the kinetic curves for the adsorption of salicylic acid on PGMA, PGMA/PDVB IPNs and PMADETA/PDVB IPNs from aqueous solution, and the initial concentration of salicylic acid was set to be 613.5 mg/L and the temperature was 298 K, respectively. It was found that the adsorption capacity of salicylic acid on the three resins increased rapidly with increasing of the adsorption time, and the adsorption reached over 85% of the equilibrium in one hour. All of the adsorption could reach equilibrium within 200 minutes, suggesting that the adsorption was a fast process. Moreover, the adsorption on PGMA could reach equilibrium in one hour, while 120 minutes were required for the adsorption on PGMA/PDVB IPNs, 180 minutes were necessary for the adsorption on PMADETA/PDVB

IPNs, suggesting that the diffusion rate of salicylic acid in the pores of PMADETA/PDVB IPNs was much slower than those of PGMA and PGMA/PDVB IPNs.

(Fig. 4 can be inserted here)

Pseudo-first-order and pseudo-second-order rate equations were applied for fitting the kinetic data [53, 54]. They can be given as:

$$\text{Pseudo-first-order rate equation: } \ln(q_e - q_t) = \ln q_e - k_1 t \quad (\text{Eq. 6})$$

$$\text{Pseudo-second-order rate equation: } t / q_t = 1 / (k_2 q_e^2) + t / q_e \quad (\text{Eq. 7})$$

where q_e and q_t (mg/g) are the equilibrium adsorption capacity and the adsorption capacity at a given time t (min), k_1 (min^{-1}) and k_2 ($\text{g}/(\text{mg}\cdot\text{min})$) are the pseudo-first-order and pseudo-second-order rate constants, respectively.

Table 4 summarizes the corresponding parameters according to the pseudo-first-order and pseudo-second-order rate equations. The adsorption on PGMA could only be fitted by the pseudo-second-order rate equation while those on PGMA/PDVB IPNs and PMADETA/PDVB IPNs could be fitted by both of the two equations due to the high correlation coefficients ($R^2 > 0.98$). In particular, the k_2 values on PGMA, PGMA/PDVB IPNs and PMADETA/PDVB IPNs were measured to be 0.0066, 0.0011, 0.0003 $\text{g}/(\text{mg}\cdot\text{min})$, accordant with the observed experimental fact that the adsorption on PGMA was the fastest while that on PMADETA/PDVB IPNs was the slowest.

(Table 4 can be inserted here)

In the adsorption of aromatic compounds on porous resin, the intra-particle diffusion process is frequently the rate-limiting step [55]. The intra-particle diffusion model can be expressed as:

$$q_t = k_p t^{0.5} \quad (\text{Eq. 8})$$

where k_p is the intra-particle diffusion rate parameter.

By employing the intra-particle diffusion model to fit the kinetic data and Fig. 4 (b) is the

plotting of the q_t versus $t^{0.5}$. The plotting showed similar characters having two linear segments followed by a plateau. In the first stage, plotting of q_t versus $t^{0.5}$ gave a straight line and the straight line passes through the origin, which suggested that the intra-particle diffusion was the only rate-limited step. In particular, the k_p on PGMA, PGMA/PDVB IPNs and PMADETA/PDVB IPNs were linearly fitted to be 6.35, 7.02 and 17.01, respectively, which was different from the average k_2 values in Table 4.

3.4 Dynamic adsorption and desorption

Fig. 5 displays the dynamic curves for the adsorption and desorption of salicylic acid on PMADETA/PDVB IPNs resin column. Here $C/C_0=0.05$ (where C is the concentration of salicylic acid from the effluent, mg/L) is defined as the breakthrough point and the volume of the effluent to reach this point is identified as V_b . The volume of the effluent to reach the saturated point is identified as V_s and $C/C_0=0.95$ is defined as the saturated adsorption point. Fig. 5 indicates that V_b and V_s were measured to be 72.42 and 154.0 BV at an initial concentration of 1035 mg/L and a flow rate of 9.8 BV/h, and the corresponding adsorption capacities the breakthrough point and the saturated adsorption point could be calculated to be 75.02 and 159.53 mg/mL wet resin, respectively.

(Fig. 5 can be inserted here)

After the dynamic adsorption, different solvents were selected for the desorption process, and the desorption ratios of PMADETA/PDVB IPNs resin column by different solvents are displayed in Fig. 6 (a). It is evident that water can hardly desorb salicylic acid from the resin column and only 29.71% of salicylic acid was desorbed from the resin column as water was applied as the desorption solvent. Meanwhile, NaOH aqueous solution was effective for desorption of salicylic acid from the resin column and 96.2% of salicylic acid could be recovered by 0.01 mol/L of NaOH (w/v). Moreover, adding some quantities of ethanol in 0.01 mol/L of NaOH (w/v) could favorably increase the desorption ratio, and a mixed desorption

solvent containing 0.01 mol/L of NaOH (w/v) and 20% of ethanol (v/v) could completely desorb salicylic acid from the resin column, and the desorption ratio reached 99.6%. Hence, 0.01 mol/L of NaOH (w/v) and 20% of ethanol (v/v) was applied as the desorption solvent in the dynamic desorption process. At a flow rate of 3.5 BV/h, only 27.0 BV of the desorption solvent was shown to be enough for complete regeneration of the resin column, and the dynamic desorption capacity was calculated to be 820.6 mg, which was excellently coincident with the dynamic capacity (826.9 mg). PMADETA/PDVB IPNs were repeatedly used for five cycles of continuous adsorption-desorption process, and the result indicated that PMADETA/PDVB IPNs exhibit good reusability with remarkable regeneration behaviors (Fig. 6 (b)).

(Fig. 6 can be inserted here)

4. Conclusions

We synthesized macroporous crosslinked PMADETA/PDVB IPNs by filling PDVB networks in the pores of PGMA networks and following by an amination reaction of the obtained macroporous crosslinked PGMA/PDVB IPNs with DETA. The synthesized PMADETA/PDVB IPNs was both hydrophilic and hydrophobic, which led a very large equilibrium adsorption capacity to salicylic acid containing hydrophilic and hydrophobic portion. The equilibrium adsorption capacity of salicylic acid on PMADETA/PDVB IPNs was 196.4 mg/g at an equilibrium concentration of 100 mg/L and 298 K, the Freundlich model was more appropriate for fitting the equilibrium data than the Langmuir model and the thermodynamic parameters were all negative. The pseudo-second-order rate equation was more suitable for characterizing the kinetic data than the pseudo-first-order rate equation and the adsorption in the first process could be fitted by the intra-particle diffusion model. The breakthrough and saturated dynamic adsorption capacities were measured to be 75.02 and

159.53 mg/mL wet resin at an initial concentration of 1035 mg/L and a flow rate of 9.8 BV/h, and the resin column could be completely regenerated by 0.01 mol/L of NaOH (w/v) and 20% of ethanol (v/v).

Acknowledgements

The National Natural Science Foundation of China (No. 21174163, 21376275 and 21446016) and South Wisdom Valley Innovative Research Team Program are gratefully acknowledged for the financial support.

References

- [1] A. Judefeind, P.J. van Rensburg, S. Langelaar and J. du Plessis, Stable isotope dilution analysis of salicylic acid and hydroquinone in human skin samples by gas chromatography with mass spectrometric detection, *J. Chromatogr. B*, 2007, 852, 300-307.
- [2] M.T. Jafari, Z. Badihi and E. Jazan, A new approach to determine salicylic acid in human urine and blood plasma based on negative electrospray ion mobility spectrometry after selective separation using a molecular imprinted polymer, *Talanta*, 2012, 99, 520-526.
- [3] N. Misra and P. Saxena, Effect of salicylic acid on proline metabolism in lentil grown under salinity stress, *Plant Sci.*, 2009, 177, 181-189.
- [4] J. Araña, E.P. Melián, L.V.M. Rodríguez, A.A. Peña, R.J.M. Doña, D.O. González and P.J. Pérez, Photocatalytic degradation of phenol and phenolic compounds: Part I. Adsorption and FTIR study, *J. Hazard. Mater.*, 2007, 146, 520-528.
- [5] M.J. Meng, Y.H. Feng, M. Zhang, Y. Liu, Y.J. Ji, J. Wang, Y.L. Wu and Y.S. Yan, Highly efficient adsorption of salicylic acid from aqueous solution by wollastonite-based imprinted adsorbent: a fixed-bed column study, *Chem. Eng. J.*, 2013, 225, 331-339.
- [6] Q. Hayata, S. Hayata, M. Irfana and A. Ahmad, Effect of exogenous salicylic acid under changing environment: a review, *Environ. Exp. Bot.*, 2010, 68, 14-25.

- [7] L.S. María, M. Andrés, D. Herminia and C.P. Juan, Recovery, concentration and purification of phenolic compounds by adsorption: a review, *J. Food Eng.*, 2011, 105, 1-27.
- [8] M. Farré, I. Ferrer, A. Ginebreda, M. Figueras, L. Olivella, L. Tirapu, M. Vilanova and D. Barceló, Determination of drugs in surface water and wastewater samples by liquid chromatography–mass spectrometry: methods and preliminary results including toxicity studies with *Vibrio fischeri*, *J. Chromatogr. A*, 2001, 938, 187-197.
- [9] E. Díaz, J.I. Jiménez and J. Nogales, Aerobic degradation of aromatic compounds, *Curr. Opin. Biotechnol.*, 2013, 24, 431-442.
- [10] M.D. Marsolek, M.J. Kirisits, K.A. Gray and B.E. Rittmann, Coupled photocatalytic-biodegradation of 2, 4, 5-trichlorophenol: Effects of photolytic and photocatalytic effluent composition on bioreactor process performance, community diversity, and resistance and resilience to perturbation, *Water Res.*, 2014, 50, 59-69.
- [11] P. Veverka and K. Jeřábek, Mechanism of hypercrosslinking of chloromethylated styrene-divinylbenzene copolymers, *React. Funct. Polym.*, 1999, 41, 21-25.
- [12] C.L. Zhang, L. Wu, D.Q. Cai, C.Y. Zhang, N. Wang, J. Zhang and Z.Y. Wu, Adsorption of polycyclic aromatic hydrocarbons (fluoranthene and anthracenemethanol) by functional graphene oxide and removal by pH and temperature-sensitive coagulation, *ACS Appl. Mater. Inter.*, 2013, 5, 4783-4790.
- [13] E.V. Lau, S. Gan, H.K. Ng and P.E. Poh, Extraction agents for the removal of polycyclic aromatic hydrocarbons (PAHs) from soil in soil washing technologies, *Environ. Pollut.*, 2014, 184, 640-649.
- [14] I. Urruzola, L. Serrano, R. Llano-Ponte, A.M. Angeles and J. Labidi, Obtaining of eucalyptus microfibrils for adsorption of aromatic compounds in aqueous solution, *Chem. Eng. J.*, 2013, 229, 42-49.

- [15] X.Y. Jin and J.H. Huang, Adsorption of vanillin by an anisole-modified hyper-cross-linked polystyrene resin from aqueous solution: equilibrium, kinetics, and dynamics, *Adv. Polym. Tech.*, 2013, 32, 221-230.
- [16] D.D. Do, Adsorption analysis, World Scientific, 1998.
- [17] J.H. Huang, L. Yang, X.M. Wang, H.B. Li, L.M. Chen and Y.N. Liu, A novel post-cross-linked polystyrene/polyacryldiethylenetriamine (PST_pc/PADETA) interpenetrating polymer networks (IPNs) and its adsorption towards salicylic acid from aqueous solutions, *Chem. Eng. J.*, 2014, 248, 216-222.
- [18] X.M. Wang, L.M. Chen, Y.N. Liu and J.H. Huang, Macroporous crosslinked polydivinylbenzene/polyacryldiethylenetriamine (PDVB/PADETA) interpenetrating polymer networks (IPNs) and their efficient adsorption to *o*-aminobenzoic acid from aqueous solutions, *J. Colloid Interf. Sci.*, 2014, 429, 83-87.
- [19] B. Saha, R.J. Gill, D.G. Bailey, N. Kabay and M. Arda, Sorption of Cr(VI) from aqueous solution by Amberlite XAD-7 resin impregnated with Aliquat 336, *React. Funct. Polym.*, 2004, 60, 223-244.
- [20] C. Valderrama, J.I. Barios, M. Caetano, A. Farran and J.L. Cortina, Kinetic evaluation of phenol/aniline mixtures adsorption from aqueous solutions onto activated carbon and hypercrosslinked polymeric resin (MN200), *React. Funct. Polym.*, 2010, 70, 142-150.
- [21] B. Saha and M. Streat, Adsorption of trace heavy metals: application of surface complexation theory to a macroporous polymer and a weakly acidic ion-exchange resin, *Ind. Eng. Chem. Res.*, 2005, 44, 8671-8681.
- [22] D. Klemperer, L.H. Sperling and L.A. Utracki, *Interpenetrating polymer networks*, An American Chemical Society Publication, 1994.
- [23] L.H. Sperling, *Interpenetrating Polymer Networks and Related Materials*, Plenum, New York, 1981.

- [24] M. Tsumura, K. Ando, J. Kotani, M. Hiraishi and T. Iwahara, Silicon-based interpenetrating polymer networks (IPNs): Synthesis and properties, *Macromolecules*, 1998, 31, 2716-2723.
- [25] J. Zhang and N.A. Peppas, Synthesis and characterization of pH- and temperature-sensitive poly (methacrylic acid)/poly (N-isopropylacrylamide) interpenetrating polymeric networks, *Macromolecules*, 2000, 33, 102-107.
- [26] Y. Chang, S.F. Chen, Q.M. Yu, Z. Zhang, M. Bernards and S.Y. Jiang, Development of biocompatible interpenetrating polymer networks containing a sulfobetaine-based polymer and a segmented polyurethane for protein resistance, *Biomacromolecules*, 2007, 8, 122-127.
- [27] R.A. Stile and K.E. Healy, Poly(N-isopropylacrylamide)-based semi-interpenetrating polymer networks for tissue engineering applications. 1. effects of linear poly(acrylic acid) chains on phase behavior, *Biomacromolecules*, 2002, 3, 591-600.
- [28] J.H. Lee and S.C. Kim, Hydrophilic-hydrophobic interpenetrating polymer networks (IPN's) synthesized under high pressure. 1. Morphology, dynamic mechanical properties, and swelling behavior of polyurethane-polystyrene IPN's, *Macromolecules*, 1986, 19, 644-648.
- [29] S. Murayama, S. Kuroda and Z. Osawa, Hydrophobic and hydrophilic interpenetrating polymer networks composed of polystyrene and poly (2-hydroxyethyl methacrylate): 1. PS-PHEMA sequential IPNs synthesized in the presence of a common solvent, *Polymer*, 1993, 34, 2845-2852.
- [30] W.W. Liao, S.Q. Gao, X.L. Xie and M.C. Xu, Macroporous crosslinked hydrophobic/hydrophilic polystyrene/polyamide interpenetrating polymer network: Synthesis, characterization, and adsorption behaviors for quercetin from aqueous solution, *J. Appl. Polym. Sci.*, 2010, 118, 3643-3648.

- [31] X.M. Wang, X.L. Liang, J.H. Huang and Y.N. Liu, Hydrophobic–hydrophilic polydivinylbenzene/polyacryldiethylenetriamine interpenetrating polymer networks and its adsorption performance toward salicylic acid from aqueous solutions, *AIChE J.* 2014, 60, 2636-2643.
- [32] B.L. He and W.Q. Huang, *Ion exchange and adsorptive resin*, Shanghai Science and Education Press, Shanghai, 1995.
- [33] M.L. Zhang and Y. Sun, Poly(glycidyl methacrylate-divinylbenzene-triallyliso cyanurate) continuous-bed protein chromatography, *J. Chromatogra. A*, 2001, 912, 31-38.
- [34] J.T. Wang, Q.M. Hu, B.S. Zhang and Y.M. Wang, *Organic Chemistry*, Nankai University Press, Tianjing, 1998.
- [35] A.M. Li, Q.X. Zhang, G.C. Zhang, J.L. Chen, Z.H. Fei and F.Q. Liu, Adsorption of phenolic compounds from aqueous solutions by a water-compatible hypercrosslinked polymeric adsorbent, *Chemosphere*, 2002, 47, 981-989.
- [36] J.H. Huang, X.Y. Jin, J.L. Mao, B. Yuan, R.J. Deng and S.G. Deng, Synthesis, characterization, and adsorption properties of diethylenetriamine-modified hypercrosslinked resins for efficient removal of salicylic acid from aqueous solutions, *J. Hazard. Mater.*, 2012, 217-218, 406-415.
- [37] J.H. Huang, X.M. Wang, P.D. Patil, J. Tang, L.M. Chen and Y.N. Liu, Synthesis, characterization and adsorption properties of amide-modified hyper-cross-linked resin, *RSC Adv.*, 2014, 4, 41172-41178.
- [38] X.M. Wang, P.D. Patil, C.L. He, J.H. Huang and Y.N. Liu, Acetamide-modified hyper-cross-linked resin: Synthesis, characterization and adsorption performance to phenol from aqueous solution, *J. Appl. Polym. Sci.*, 2015, 132, 41597 (1-9).
- [39] X.M. Wang, K.L. Dai, L.M. Chen, J.H. Huang and Y.N. Liu, An ethanediamine-modified hypercrosslinked polystyrene resin: Synthesis, adsorption and separation properties, *Chem.*

- Eng. J.*, 2014, 242, 19-26.
- [40] M. Otero, C. A Grande and A. E Rodrigues, Adsorption of salicylic acid onto polymeric adsorbents and activated charcoal, *React. Funct. Polym.*, 2004, 60, 203-213.
- [41] M. Otero, M. Zabkova, A.E. Rodrigues, Comparative study of the adsorption of phenol and salicylic acid from aqueous solution onto nonionic polymeric resins, *Sep. Purif. Technol.*, 2005, 45, 86-95.
- [42] X.Q. Kong, M. Shan, V. Terskikh, I. Hung, Z.H. Gan and G. Wu, Solid-state O-17 NMR of pharmaceutical compounds: salicylic acid and aspirin, *J. Phys. Chem. B*, 2013, 117, 9643-9654.
- [43] Q.W. Wang, Y.H. Yang and H.B. Gao, *Hydrogen Bonding in Organic chemistry*, Tianjin University Press, Tianjin, 1983.
- [44] B.K. Paul and N. Guchhait, Geometrical criteria versus quantum chemical criteria for assessment of intramolecular hydrogen bond (IMHB) interaction: a computational comparison into the effect of chlorine substitution on IMHB of salicylic acid in its lowest energy ground state conformer, *Chem. Phys.*, 2013, 412, 58-67.
- [45] J.H. Huang, G. Wang and K.L. Huang, Enhanced adsorption of salicylic acid onto a β -naphthol-modified hyper-cross-linked poly(styrene-co-divinylbenzene) resin from aqueous solution, *Chem. Eng. J.*, 2011, 168, 715-721.
- [46] F. Wang, B.W. Liu, P.J.J. Huang and J.W. Liu, Rationally designed nucleobase and nucleotide coordinated nanoparticles for selective DNA adsorption and detection, *Anal. Chem.*, 2013, 85, 12144-12151.
- [47] W.M. Zhang, Q. Du, B.C. Pan, L. Lv, C.H. Hong, Z.M. Jiang and D.Y. Kong, Adsorption equilibrium and heat of phenol onto aminated polymeric resins from aqueous solution, *Colloids Surf. A*, 2009, 346, 34-38.
- [48] A. Hirano, T. Tanaka, Y. Urabe and H. Kataura, pH- and solute-dependent adsorption of

single-wall carbon nanotubes onto hydrogels: mechanistic insights into the metal/semiconductor separation, *ACS Nano*, 2013, 7, 10285-10295.

- [49] A. Werner and H. Hasse, Experimental study and modeling of the influence of mixed electrolytes on adsorption of macromolecules on a hydrophobic resin, *J. Chromatogr. A*, 2013, 1315, 135-144.
- [50] I. Langmuir, The constitution and fundamental properties of solids and liquids. Part I. Solids, *J. Am. Chem. Soc.*, 1916, 38, 2221-2295.
- [51] H.M.F. Freundlich, Über die adsorption in lösungen, *Z. Phys. Chem.*, 1906, 57A, 385-470.
- [52] H.T. Li, M.C. Xu, Z.Q. Shi and B.L. He, Isotherm analysis of phenol adsorption on polymeric adsorbents from nonaqueous solution, *J. Colloid. Interf. Sci.*, 2004, 271, 47-54.
- [53] S. Lagergren, About the theory of so-called adsorption of soluble substances, *Kungl. Svenska vetenskapsakademien, Handlingar*, 1898, 24, 1-39.
- [54] Y.S. Ho and G. McKay, Sorption of dye from aqueous solution by peat, *Chem. Eng. J.*, 1998, 70, 115-124.
- [55] W.J. Weber, J.C. Morris and Sanit, Kinetics of adsorption on carbon from solution, *J. Eng. Div. Am. Soc. Civ. Eng.*, 1963, 89, 31-60.

Table 1 Main structural parameters of PGMA, PMADETA, PGMA/PDVB IPNs and PMADETA/PDVB IPNs, respectively.

	PGMA	PMADETA	PGMA/PDVB IPNs	PMADETA/PDVB IPNs
BET surface area / (cm ² /g)	64.00	39.63	271.3	290.3
Pore volume / (cm ³ /g)	0.3587	0.2456	0.7249	0.8780
Particle size / (mm)	0.4-0.6	0.4-0.6	0.4-0.6	0.4-0.6
Average pore diameter / (nm)	12.06	11.11	8.896	10.32
Weak exchange capacity / (mmol/g)	—	2.898	—	3.479

Table 2 Correlative parameters of equilibrium data of salicylic acid on PMADETA/PDVB IPNs from aqueous solution according to the Langmuir and Freundlich models.

	Langmuir model					Freundlich model				
	q_m /(mg/g)	Standard Error	K_L /(L/mg)	Standard Error	R^2	K_F /([(mg/g)(L/mg) ^{1/n}])	Standard Error	n	Standard Error	R^2
298 K	232.4	14.31	0.2808	0.1400	0.9299	87.08	1.449	5.631	0.0980	0.9997
308 K	232.4	14.50	0.1209	0.0566	0.9375	73.71	1.706	4.992	0.1058	0.9995
318 K	238.3	13.20	0.0674	0.0248	0.9585	66.32	3.622	4.623	0.2131	0.9977

Table 3 Thermodynamics parameters for the adsorption of salicylic acid on PMADETA/PDVB IPNs from aqueous solution.

q_e /(mg/g)	ΔH /(kJ/mol)	Errors	ΔG /(kJ/mol)						ΔS /(J/mol·K)					
			298 K		308 K		318 K		298 K		308 K		318 K	
			Errors	Errors	Errors	Errors	Errors	Errors	Errors	Errors	Errors	Errors	Errors	
80	-53.11	±0.5	-13.95	±0.3	-12.78	±0.3	-12.22	±0.3	-131.3	±1.5	-130.9	±1.5	-128.5	±1.5
120	-36.97	±0.5	-13.95	±0.3	-12.78	±0.3	-12.22	±0.3	-77.22	±1.5	-78.51	±1.5	-77.80	±1.5
160	-25.51	±0.5	-13.95	±0.3	-12.78	±0.3	-12.22	±0.3	-38.79	±1.5	-41.32	±1.5	-41.78	±1.5
200	-16.63	±0.5	-13.95	±0.3	-12.78	±0.3	-12.22	±0.3	-8.970	±1.5	-12.47	±1.5	-13.85	±1.5

Table 4 Correlative parameters of kinetic data of salicylic acid on PGMA, PGMA/PDVB IPNs and PMADETA/PDVB IPNs from aqueous solution according to the pseudo-first-order and pseudo-second-order rate equations.

	Pseudo-first-order					Pseudo-second-order				
	q_m /(mg/g)	Standard Error	k_1 /(min ⁻¹)	Standard Error	R^2	q_m /(mg/g)	Standard Error	k_2 /(g/(mg·min))	Standard Error	R^2
PGMA	29.11	0.4649	0.1293	0.0107	0.9724	31.21	0.2525	0.0066	3.769×10^{-4}	0.9952
PGMA/PDVB IPNs	52.36	0.3252	0.0484	0.0011	0.9974	58.85	1.041	0.0011	9.710×10^{-5}	0.9875
PMADETA/PDVB IPNs	137.7	1.517	0.0385	0.0016	0.9895	155.9	0.7732	0.0003	7.927×10^{-6}	0.9988

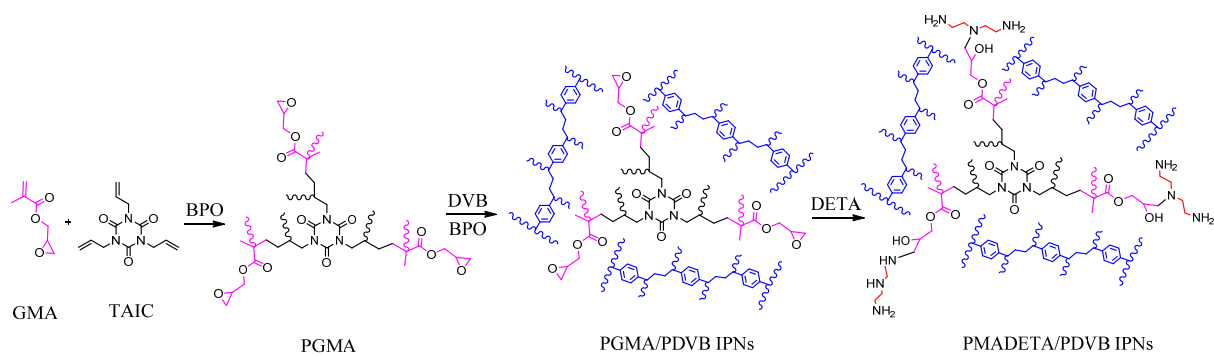
Scheme 1 Synthetic procedure of PMADETA/PDVB IPNs.

Fig. 1 FT-IR spectra of PGMA, PDVB, PMADETA, PGMA/PDVB IPNs and PMADETA/PDVB IPNs, respectively.

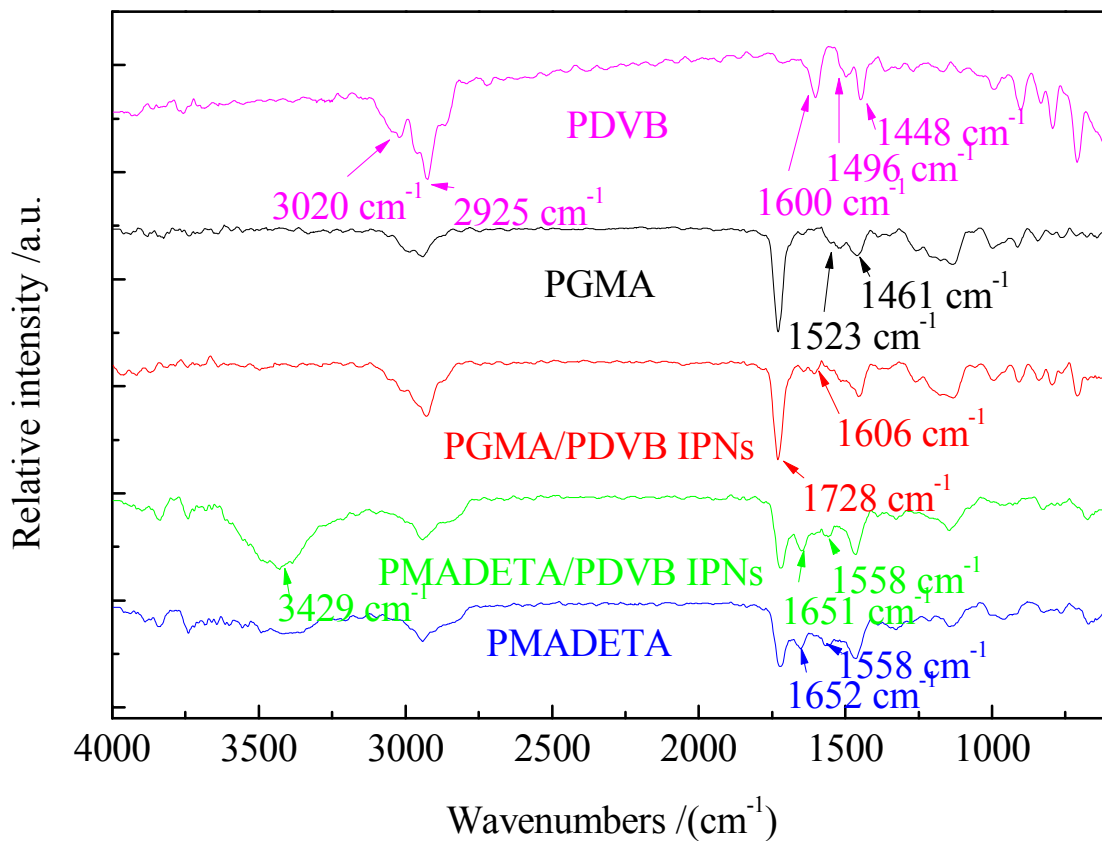


Fig. 2 Equilibrium isotherms of salicylic acid on PGMA, PMADETA, PGMA/PDVB IPNs and PMADETA/PDVB IPNs from aqueous solution with the temperature at 298 K.

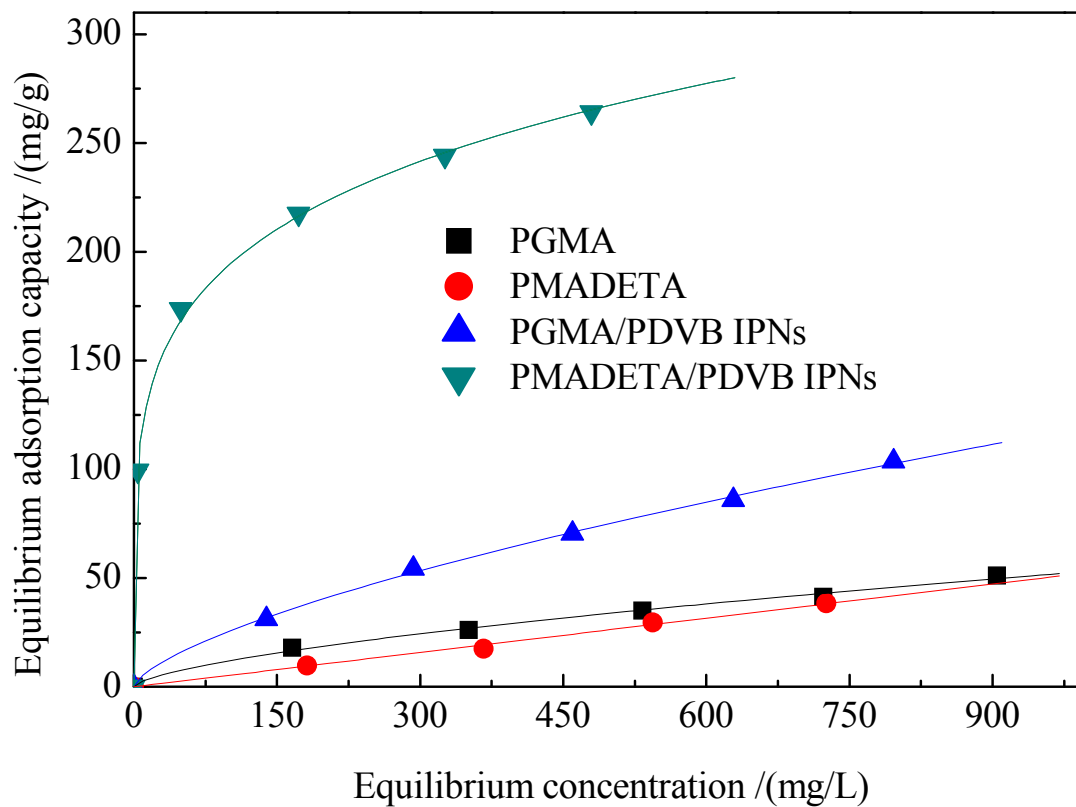


Fig. 3 Equilibrium isotherms of salicylic acid on PMADETA/PDVB IPNs from aqueous solution with the temperature at 298, 308 and 318 K, respectively.

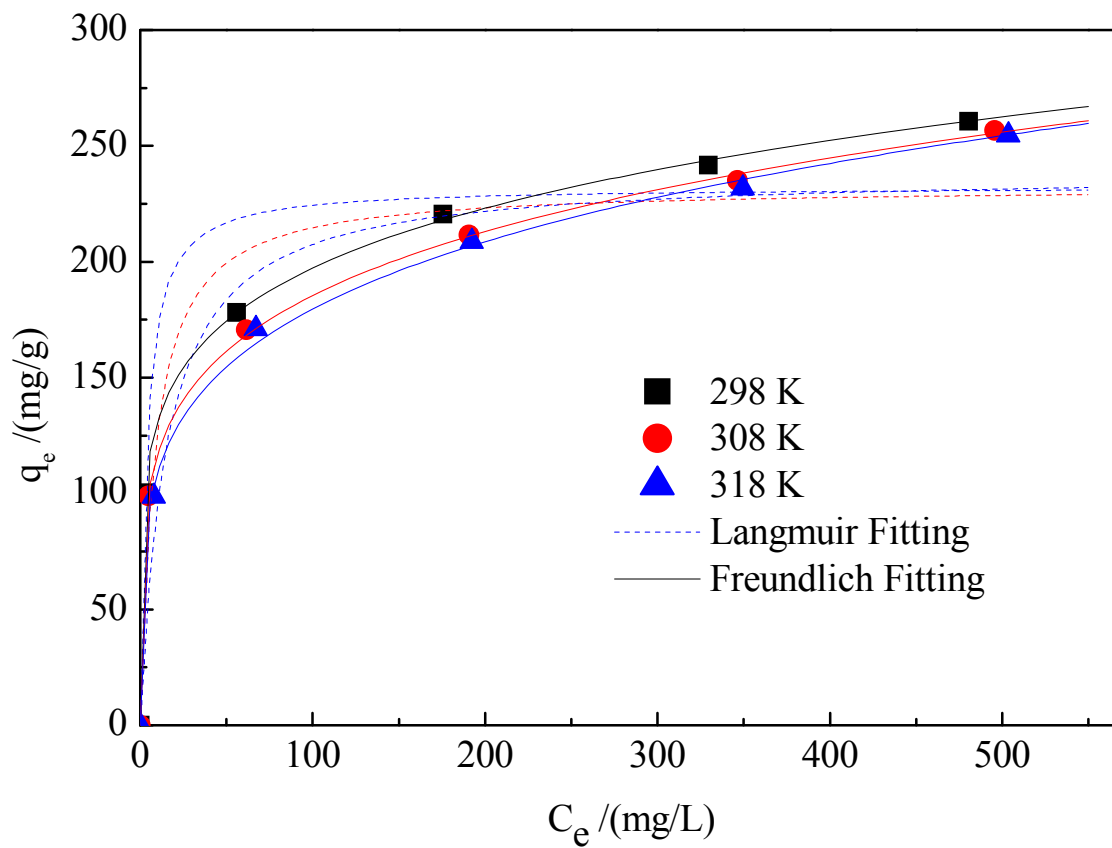


Fig. 4 (a) Kinetic adsorption curves of salicylic acid on PGMA, PGMA/PDVB IPNs and PMADETA/PDVB IPNs from aqueous solution with the temperature at 298 K and the initial concentration at 613.5 mg/L, respectively; (b) Intra-particle diffusion fitting curves of salicylic acid on PGMA, PGMA/PDVB IPNs and PMADETA/PDVB IPNs from aqueous solutions, respectively.

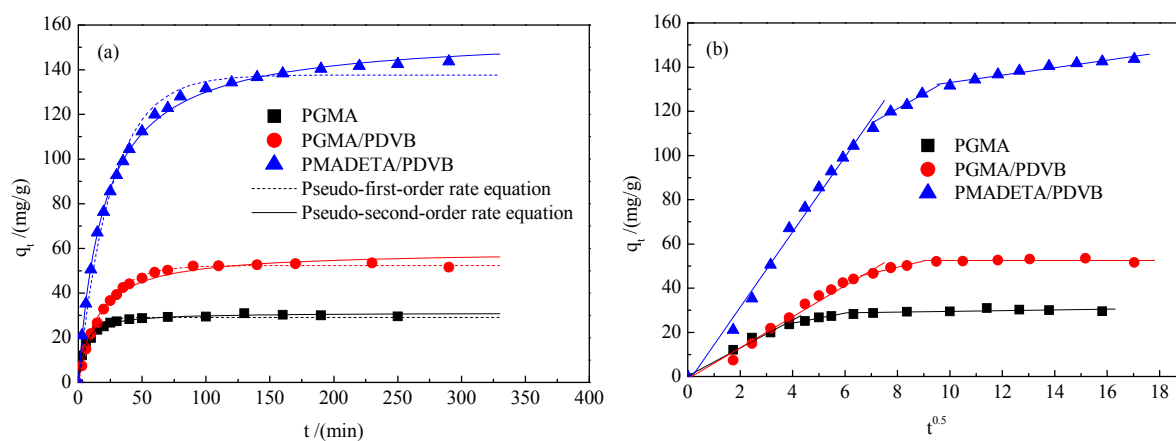


Fig. 5 Dynamic adsorption and desorption curves of salicylic acid on PMADETA/PDVB IPNs resin column from aqueous solution.

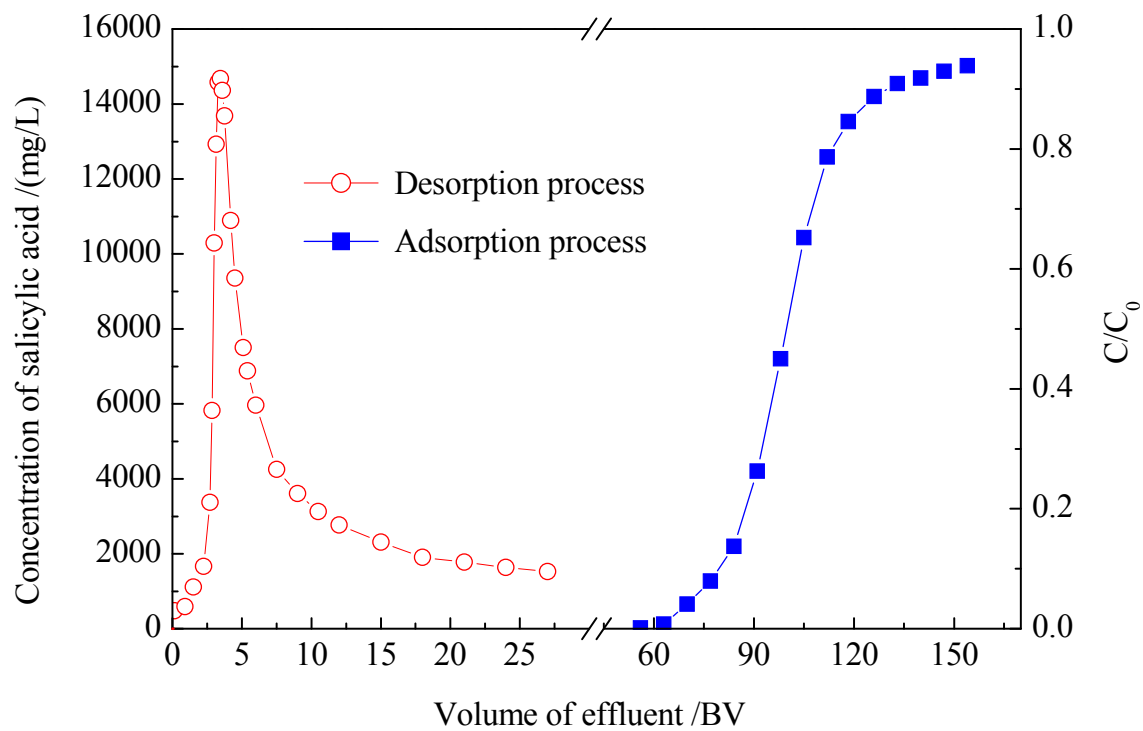


Fig. 6 (a) Static desorption ratios of salicylic acid on PMADETA/PDVB IPNs from aqueous solution. (A: deionized water; B: 20% of ethanol (v/v); C: 50% of ethanol (v/v); D: 0.01 mol/L of NaOH (w/v); E: 0.01 mol/L of NaOH (w/v) and 20% of ethanol (v/v); F: 0.01 mol/L of NaOH (w/v) and 50% of ethanol (v/v)); (b) Regeneration of the adsorption of salicylic acid on PMADETA/PDVB IPNs within five cycles.

